Peroxisome development in yeast is associated with the formation of Pex3-dependent peroxisome-vacuole contact sites

Wu, Huala; de Boer, Rinse; Krikken, Arjen M; Akşit, Arman; Yuan, Wei; van der Klei, Ida J

Published in:
Biochimica et Biophysica Acta (BBA) - Molecular Cell Research

DOI:
10.1016/j.bbamcr.2018.08.021

Publication date:
2019

BBA - Molecular Cell Research 1866 (2019) 349–359

Contents lists available at ScienceDirect

BBA - Molecular Cell Research

journal homepage: www.elsevier.com/locate/bbamcr

Peroxisome development in yeast is associated with the formation of Pex3-dependent peroxisome-vacuole contact sites

Huala Wu, Rinse de Boer, Arjen M. Krikken, Arman Akşit, Wei Yuan[1], Ida J. van der Klei*

Molecular Cell Biology, University of Groningen, PO Box 11103, 9300, CC, Groningen, the Netherlands

ARTICLE INFO

Keywords:
Yeast
Peroxisome
Vacuole
Contact sites
Pex3

ABSTRACT

Using electron and fluorescence microscopy techniques, we identified various physical contacts between peroxisomes and other cell organelles in the yeast *Hansenula polymorpha*.

In exponential glucose-grown cells, which typically contain a single small peroxisome, contacts were only observed with the endoplasmic reticulum and the plasma membrane. Here we focus on a novel peroxisome-vacuole contact site that is formed when glucose-grown cells are shifted to methanol containing media, conditions that induce strong peroxisome development. At these conditions, the small peroxisomes rapidly increase in size, a phenomenon that is paralleled by the formation of distinct intimate contacts with the vacuole.

Localization studies showed that the peroxin Pex3 accumulated in patches at the peroxisome-vacuole contact sites. In wild-type cells growing exponentially on medium containing glucose, peroxisome-vacuole contact sites were never observed. However, upon overproduction of Pex3 peroxisomes also associated to vacuoles at these growth conditions.

Our observations strongly suggest a role for Pex3 in the formation of a novel peroxisome-vacuole contact site. This contact likely plays a role in membrane growth as it is formed solely at conditions of strong peroxisome expansion.

1. Introduction

For long, cell organelles were assumed to represent compartments that function in relative isolation, but now we know that they intimately collaborate in several important cellular processes. These collaborations not only involve functional interactions but also include tight physical associations between organelles. Well-established roles of organellar contacts are lipid [1] and calcium transport [2]. Tight physical contacts between organelles are not only important for the transport of small molecules but also play a role in various other processes such as organelle fission, movement and autophagy. Recent studies showed that virtually all organelles form contacts with other cell compartments. A striking example is the endoplasmic reticulum (ER), which associates with mitochondria, peroxisomes, vacuoles, lipid bodies, the Golgi apparatus, (auto)phagosomes and the plasma membrane (for a review see [3]).

Our knowledge on the occurrence, composition and function of peroxisomal contacts is still in its infancy [4]. Peroxisomes are ubiquitous organelles that play important roles in a range of metabolic and non-metabolic functions [5]. At the morphological level, associations between peroxisomes and other cellular membranes are already known for several decades (reviewed in [6]). Recently, the first functions of peroxisomal contact sites as well as proteins that are localized to these sites were identified. For instance, in mammals, peroxisome-ER contacts have been described that play a role in lipid transport [7,8]. In yeast, ER-peroxisome contacts play a role in peroxisome retention. This contact requires Inp1, which simultaneously binds ER- and peroxisome-bound Pex3 [9,10]. Another yeast peroxisome-ER contact involves the ER resident proteins Pex29 and Pex30, which form a complex with the ER-localized reticulon homology proteins Rtn1, Rtn2, and Yop1 [11–13]. This so-called EPCONS has been implicated to function in de novo peroxisome formation. Whether specific peroxisomal (tethering) proteins are involved in the formation of EPCONS is not yet known. Peroxisome-mitochondrial associations enhance metabolism by creating a short distance allowing efficient transport of metabolites between both organelles. Tethering proteins that have been identified to occur at these sites are the Peroxisomal Membrane Proteins (PMPs) Pex11 and Pex34 as well as the mitochondrial proteins Mdm34 and Fzo1 [14–16]. Moreover, contacts between peroxisomes and the autophagosomal membrane or vacuolar membrane are formed during

* Corresponding author.
E-mail address: I.J.van.der.klei@rug.nl (I.J. van der Klei).
[1] Current address: College of Biotechnology and Engineering, Zhejiang University of Technology, Zhejiang 311,122, China.

https://doi.org/10.1016/j.bbamcr.2018.08.021
Received 24 May 2018; Received in revised form 28 August 2018; Accepted 30 August 2018
Available online 01 September 2018
0167-4889/

peroxisome degradation by macro- or micropexophagy, respectively [17]. During macropexophagy, peroxisome bound Atg30 (in *Pichia pastoris*) or Atg36 (in *Saccharomyces cerevisiae*) associate with the autophagy cargo receptor Atg11 that is localized to the sequestering phagophore. PpAtg30 and ScAtg36 are recruited to peroxisomes by Pex3 (for a review see [18]).

Here we describe a detailed microscopy analysis of vacuole-peroxisome contact sites (VAPCONS) in the yeast *Hansenula polymorpha*. At peroxisome repressing growth conditions (glucose) *H. polymorpha* cells generally contain a single, small peroxisome. This organelle rapidly expands upon a shift of the cells to methanol containing media (peroxisome inducing conditions) [19]. We show that in exponential, glucose-grown inoculum cells the relatively small peroxisome only forms contacts with the plasma membrane and endoplasmic reticulum (ER), whereas shortly after the shift of cells to methanol media extensive physical contacts with vacuoles are formed as well. These contacts are developed in cells in which peroxisomes rapidly expand and are not subject to pexophagy. Hence, these novel contacts may function in the growth of the peroxisomal membrane.

Further analysis revealed that at peroxisome inducing conditions the PMP Pex3 is enriched in patches at the peroxisome-vacuole contact sites. Moreover, the formation of these structures is promoted at conditions of Pex3 overproduction.

Taken together our data suggest that *H. polymorpha* Pex3 plays a role in the formation of a novel peroxisome-vacuole contact site.

2. Results

2.1. Peroxisomes form physical contacts with different cell organelles

Yeast peroxisomes lack enzymes that synthesize membrane lipids. Therefore peroxisomal membrane lipids are derived from other cellular locations. Previous data indicated that in *S. cerevisiae* peroxisomes can receive lipids from the ER via non-vesicular transport, a process that is likely to occur at membrane contact sites [20]. Also, data have been presented showing that yeast peroxisomes may derive their membrane lipids from the ER, the Golgi apparatus, vacuoles and mitochondria [21,22]. We reasoned that potential contacts involved in lipid transfer to the peroxisomal membrane could best be identified in cells containing rapidly expanding peroxisomes. In *H. polymorpha*, these conditions are ideally met in cells, which are pre-cultivated on glucose and shifted for a few hours to medium containing methanol. *H. polymorpha* cells growing exponentially on glucose generally contain a single small peroxisome (approximately 0.1 μm in diameter) that rapidly develops into a larger organelle (almost 1 μm in diameter) before fission occurs in the first 8 h of adaptation of cells to growth on methanol [23]. Hence, the membrane surface of this peroxisome increases almost 100-fold in the same time interval.

At membrane contact sites the distance between two membranes is typically < 30 nm [3], which is far below the resolution limit of Fluorescence Microscopy (FM; 200 nm). We therefore initiated our studies with a detailed Electron Microscopy (EM) analysis. Analysis of $KMnO_4$-fixed cells shifted for 4–6 h from glucose to methanol medium confirmed that most cells contained a single enlarged peroxisome, which is the result of growth of the original small peroxisome present in the glucose-grown inoculum cells. These growing peroxisomes displayed intimate contacts with the ER, vacuoles, mitochondria and the plasma membrane (Fig. 1A). These contacts were also observed upon cryofixation of the cells (Fig. 1B), indicating that they did not represent artifacts due to the chemical fixation procedures.

Similar studies using glucose-grown control wild-type cells revealed that the single small peroxisomes present in these cells lacked vacuole contacts and were only associated with the ER and plasma membrane (Fig. 1C).

In $KMnO_4$-fixed cells, regions where the distance between the peroxisomal membrane and another membrane was < 5 nm were regularly observed. This distance was therefore used as a criterion to quantify the contacts. Analysis of series of serial sections of 10 randomly taken glucose-grown cells showed that all 10 peroxisomes in these cells were associated with the ER and frequently also with the plasma membrane, whereas none of them formed a contact with mitochondria or vacuoles. However, in methanol-induced cells, most peroxisomes formed contacts with the vacuole, ER and plasma membrane, whereas infrequently a close association of a peroxisome with a mitochondrion was observed (Fig. 1D). Measurements of the average maximum length of the different contacts revealed that in methanol-grown cells the contacts with the vacuoles were most extensive (approximately 250 nm, Fig. 1BII, Fig. 1D). Vacuoles were never observed to completely surround the peroxisomes, indicating that at these conditions of rapid organelle expansion micropexophagy did not occur. Also, peroxisomes sequestered by autophagosomes were never observed. This was the expected result as in *H. polymorpha* micropexophagy strictly depends on N-starvation, whereas macropexophagy is induced by the addition of excess glucose to methanol cultures, conditions which are not met in our experimental set up [24].

2.2. Peroxisome-vacuole contacts are formed under conditions of peroxisome growth

FM analysis of living cells confirmed that upon shifting WT cells from glucose to methanol the percentage of peroxisomes (marked with the green peroxisomal matrix marker GFP-SKL) that was associated to vacuoles (i.e. partial overlap with the red fluorescent vacuole marker FM4–64) rapidly increased to almost 100% in a time interval of 8 h (Fig. 2). At 8 h after the shift, the first peroxisome fission events were observed. At this stage vacuole-peroxisome contacts still were evident (Fig. 2A, 8 h). Also, at 16 h, when peroxisome multiplication had occurred and clusters of peroxisomes were formed, most peroxisomes were still in contact with the vacuole (Fig. 2). However, among the clustered peroxisomes not all of them formed a contact with vacuoles, resulting in a slightly decreased percentage of peroxisome-vacuole contacts at 16 h (Fig. 2B).

FM suggested that approximately 15% of the peroxisomes associated with vacuoles in glucose-grown control cells, which seems at odds with the results of the EM analysis (compare Fig. 1D). However, this can be explained by the resolution limit of FM (200 nm), which will reveal overlap of both organelle markers also when they are separated by a distance larger than 5 nm, but < 200 nm.

Our FM observations were confirmed in cryo-fixed cells (Fig. 2C), which showed that at $T = 0$ h peroxisomes were not associated with vacuoles, whereas close associations were observed in samples taken at 4, 8 or 16 h after the shift. At later time-points (8 h and 16 h) vacuoles often appeared fragmented, but remained associated with the peroxisome (Fig. 2C; 8 h). Long vacuolar protrusions that fully sequestered the peroxisome, as is typical for micropexophagy, or autophagosomes were never observed.

2.3. Pex3 accumulates in patches at peroxisome-vacuole contacts

In order to identify proteins involved in the formation of peroxisome-vacuole contacts, we tested whether specific PMPs enrich at these sites in cells induced for a few hours on methanol. In line with earlier observations, Pmp47-GFP fluorescence showed an even distribution over the entire peroxisomal periphery (Fig. 3A) [25]. Pmp47 is homologous to the *S. cerevisiae* ATP transporter Ant1 [26]. A similar pattern was observed for Pex11-GFP, an abundant PMP implicated in peroxisome fission [27], but also in the formation of peroxisome-mitochondria contacts [15]. Next, we analyzed Pex14-GFP, a component of the receptor docking complex. Pex14-GFP was observed at the entire organelle surface, but also partially enriched in patches. These patches were absent at regions where peroxisomes formed contacts with vacuoles (Fig. 3B, D). On the other hand, Pex3, a peroxin implicated in

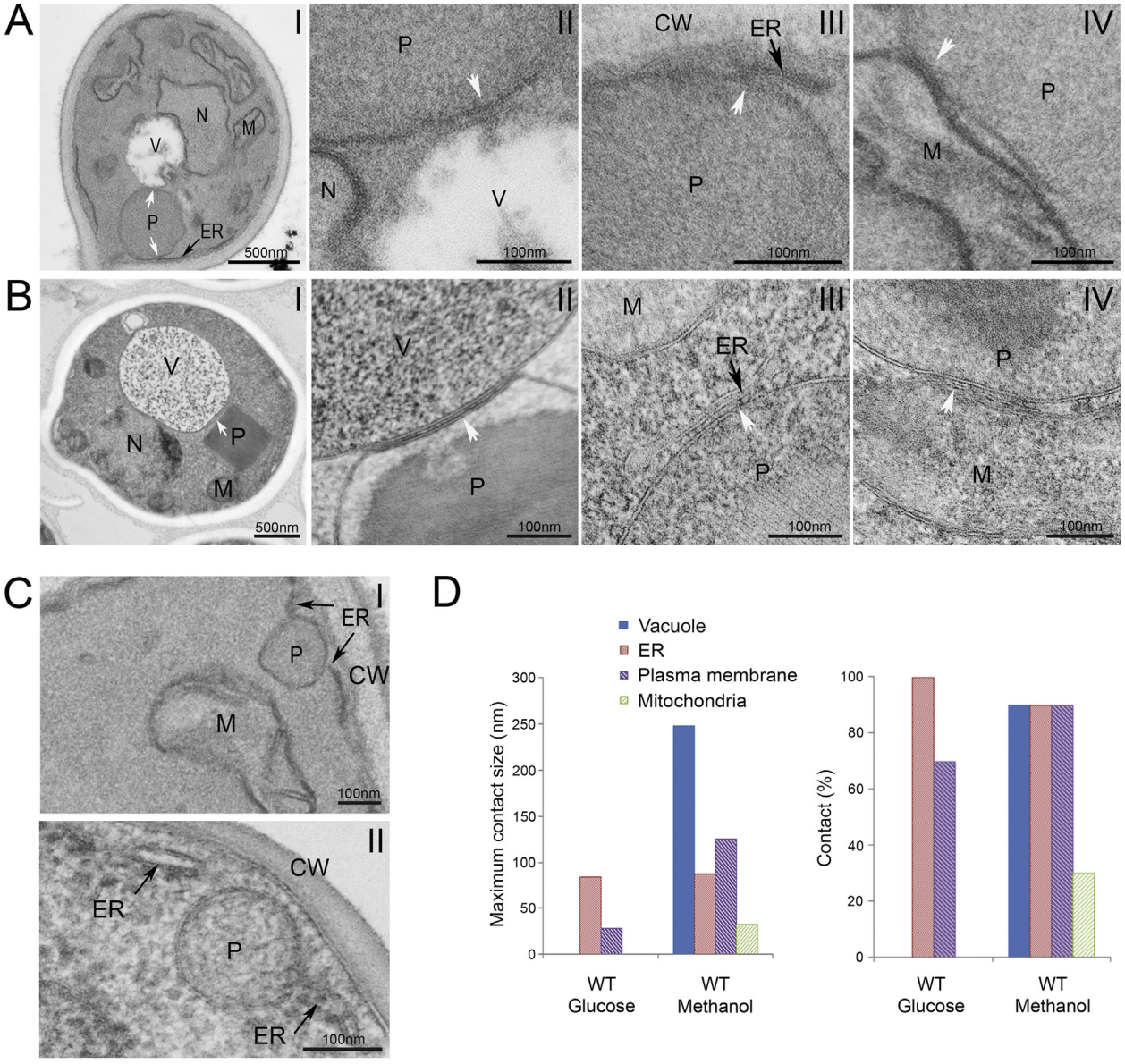

Fig. 1. Peroxisome contacts in WT *H. polymorpha* cells. (A) EM analysis of thin sections of chemically fixed ($KMnO_4$) WT cells induced for several hours on methanol medium. White arrows indicate regions where the distance between the two membranes is < 5 nm. Overview (I) and details of contacts between the peroxisome and vacuole (II), ER (III) and mitochondrion (A-IV). (B) Electron micrographs of cryofixed cells, showing an overview (I) and details of contacts with the vacuole (II), ER (III) and a mitochondrion (IV). (C) Electron micrograph of KMnO4 fixed (I) and cryofixed (II) glucose-grown WT cell showing close associations between peroxisomes with the ER and plasma membrane. (D) Quantification of contact sites in chemically fixed WT cells grown on glucose or methanol medium. The average maximum contact lengths were calculated for 10 individual peroxisomes (either of glucose- or methanol-grown cells) using a series of serial sections that comprise the entire peroxisome. For the same 10 peroxisomes, the percentage of peroxisomes containing vacuole, ER and mitochondrial contacts were quantified ($n = 10$). CW – cell wall, ER - endoplasmic reticulum, M – mitochondrion, N – nucleus, P – peroxisome, V – vacuole.

PMP sorting, also formed patches, generally one or two per organelle (Fig. 3 A, B, C, E), one of which invariably was localized at the peroxisome-vacuole contact. To further substantiate that Pex3 was localized at the contacts between peroxisomes and vacuoles, we performed correlative light and electron microscopy (CLEM). This method allows performing a detailed morphological analysis by EM of fluorescent structures identified by FM. EM analysis confirmed that invariably close contacts between the peroxisomal and vacuolar membrane were present at Pex3-GFP patches observed by FM (Fig. 3F).

Subsequently, we tested whether peroxisome-vacuole and Pex3-GFP patches still remained at peroxisome-vacuole contacts upon shifting cells from methanol-containing medium back to medium with glucose or medium without any carbon source (Fig. 4). WT cells producing GFP-SKL or Pex3-GFP were cultivated on methanol for 6 h and subsequently shifted to the indicated growth media and analyzed after 2 h.

Upon a shift to glucose medium small peroxisomes appeared, which were not attached to the vacuole, whereas the larger peroxisomes that were still observed in some of the cells remained associated with vacuoles (Fig. 4A). Pex3-GFP patches remained present at these peroxisome-vacuole contacts after the addition of glucose (Fig. 4B). Quantitative analysis revealed that indeed the percentage of peroxisomes associated with vacuoles strongly decreased (Fig. 4C). Upon a shift to media without methanol, no obvious changes in peroxisome-vacuole contacts or Pex3-GFP patches were observed.

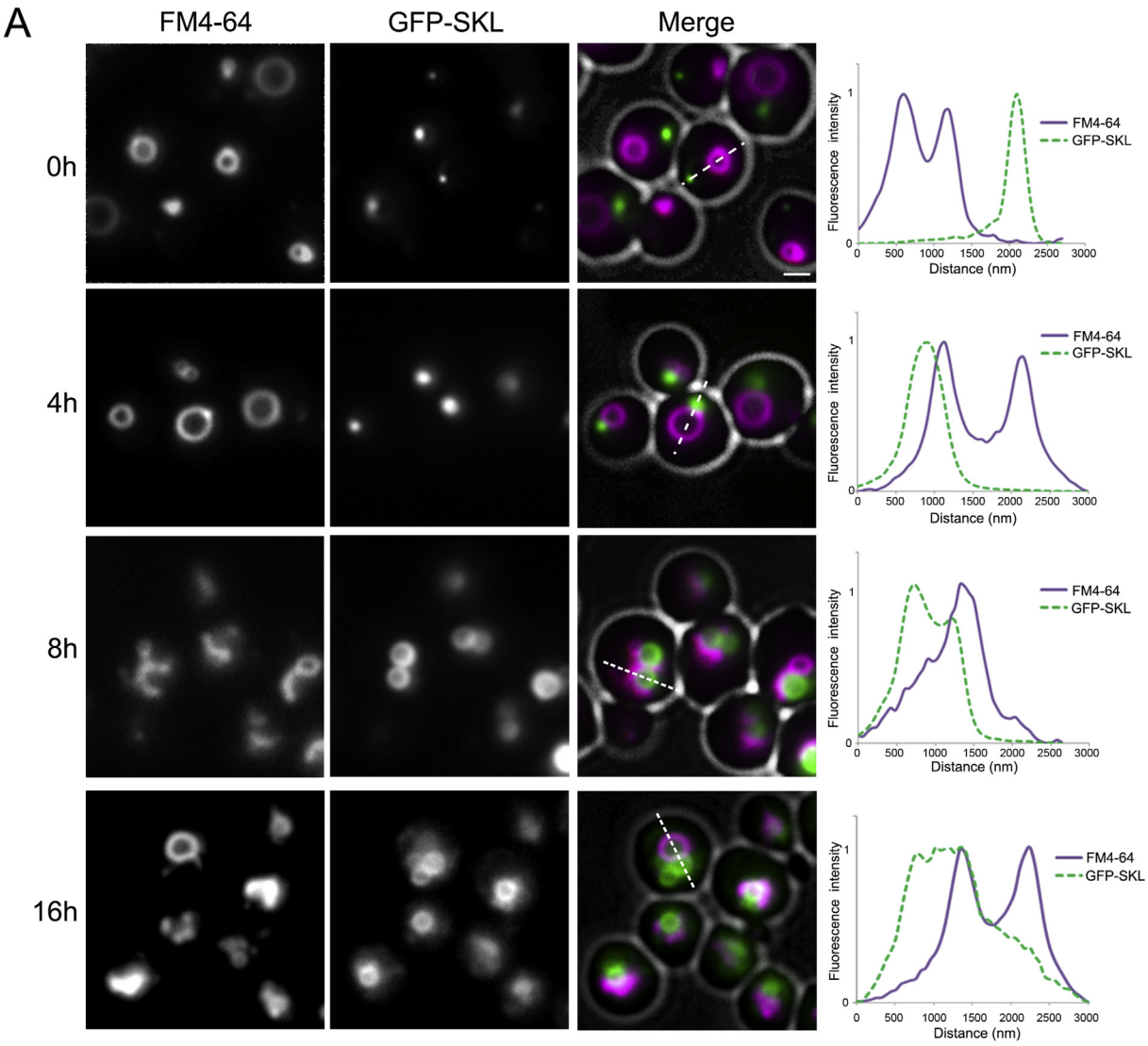

(caption on next page)

Fig. 2. Close associations of peroxisome and vacuoles are formed upon induction of peroxisome development. (A) Fluorescence microscopy images of WT cells shifted from glucose (T – 0 h) to methanol medium for 4, 8 h or 16 h. Cells produce the peroxisomal matrix marker GFP-SKL. Vacuoles are stained with FM4–64. Scale bar 1 μm. Graphs show normalized fluorescence intensity along the lines indicated in the merged images. (B) Percentage of peroxisomes that form peroxisome-vacuole contacts at the indicated time points (see A). Peroxisome-vacuole contacts were defined as regions where green fluorescence signals (from GFP-SKL) overlapped with red fluorescence from FM4-64. Error bars represent standard deviation (SD). 200 peroxisomes of two independent cultures were used for the quantification. $^{*}p < 0.05$, *t*-test. (C) Electron micrographs of cryofixed cells at the indicated time points after the shift of glucose-grown cells to methanol containing medium. M – mitochondrion, N – nucleus, P – peroxisome, V – vacuole.

2.4. Overproduction of Pex3 stimulates the formation of peroxisome-vacuole contact sites in glucose-grown cells

Next, we analyzed whether Pex3 may play a direct role in the formation of peroxisome-vacuole contacts. Because these contacts are absent in cells grown on glucose (Fig. 1D), we tested whether overproduction of Pex3-GFP in glucose-grown cells would lead to the formation of peroxisome-vacuole contacts. A strain overproducing Pex14-GFP was used as a control. In order to obtain overproduction, *PEX3-GFP* or *PEX14-GFP* were placed under control of the relatively strong amine oxidase promoter (P_{AMO}). These strains, (called $Pex3^{++}$ or $Pex14^{++}$), together with control strains producing Pex3-GFP or Pex14-GFP under control of the endogenous promoters, were grown on media containing glucose/methylamine to induce P_{AMO}. As shown in Fig. 5A, B in $Pex3^{++}$ cells, an increased number of peroxisome-vacuole contacts was observed, relative to the WT control. In the control experiment using $Pex14^{++}$ an increase in peroxisome-vacuole contact sites was not observed (Fig. 5A–E). In these cells often multiple peroxisomes were observed because Pex14 overproduction stimulates peroxisome proliferation (Komori et al., 1997). Western blot analysis confirmed that Pex3-GFP and Pex14-GFP levels were enhanced in glucose/methylamine grown $Pex3^{++}$ and $Pex14^{++}$ cells (Fig. 5C).

In FM images, 30% of the peroxisomes showed overlap with the FM4–64 marker in the glucose/methylamine grown WT control. This slightly enhanced percentage (compare Fig. 2) is most likely related to moderate peroxisome growth due to the import of the peroxisomal enzyme amine oxidase and the increased size of vacuoles at these growth conditions [28].

EM analysis confirmed that vacuole-peroxisome contacts did not occur in WT and $Pex14^{++}$ cells grown on glucose/methylamine, whereas approximately 40% of the peroxisomes in the $Pex3^{++}$ strain were closely associated with vacuoles (distance < 5 nm) (Fig. 5D, E).

3. Discussion

Here we describe a novel peroxisome-vacuole contact in yeast that develops under conditions of rapid peroxisome development. Our data indicate that the PMP Pex3 is involved in the formation of this contact.

Peroxisome-vacuole contacts have been described before and occur in *H. polymorpha* at conditions of nitrogen starvation, which induces micropexophagy, where extensions of the vacuole enclose the organelle to be degraded [24]. At the experimental conditions used in our current studies, all nutrients are present in excess. Indeed, our EM analysis revealed that peroxisomes were never engulfed by vacuolar extensions or taken up in vacuoles, as is typical for micropexophagy, in the early exponential methanol cultures.

The peroxisome-vacuole contacts we identified are also not related to macropexophagy. During macropexophagy peroxisomes are first enclosed by the autophagosomal membrane, which subsequently fuses with the vacuole. Hence, in macropexophagy, direct contacts between the peroxisomal and vacuolar membrane do not occur. Also, in *H. polymorpha* macropexophagy is characteristically induced upon a shift of methanol-grown cells to glucose-excess conditions [29], but never observed in cells in the exponential growth phase on methanol.

We analyzed *H. polymorpha* cells in which peroxisome growth and proliferation are massively induced. Possibly, the peroxisome-vacuole contact formed at these conditions may play a role in non-vesicular lipid transport from the vacuolar to the peroxisomal membrane. Notably, in *S. cerevisiae* phosphatidylethanolamine (PE) synthesized by phosphatidylserine decarboxylase 2 (Psd2) is transferred to the peroxisomal membrane [22]. Because Psd2 is localized to Golgi and vacuole membranes it is tempting to speculate that PE produced at the vacuole membrane is directly transported to peroxisomal membranes at vacuole-peroxisome contact sites. Lipid transport from the vacuolar membrane to other organelles indeed can occur in yeast, for instance to mitochondria at a contact site called vCLAMP (vacuole and mitochondria patch) [30–32].

We showed that Pex3 accumulates in patches at peroxisome-vacuole contact sites (Fig.3). Moreover, overproduction of this peroxin resulted in the formation of peroxisome-vacuole contact sites at conditions, where these sites normally do not occur (glucose medium, peroxisome repressing growth conditions) (Fig. 5). These results indicate that Pex3 is a crucial protein for the formation of the peroxisome-vacuole contact sites. In addition, these data imply that methanol is not an essential signaling molecule for the formation of the contact sites. This is underscored by the observation that the contact sites are preserved upon a shift of methanol-grown cells to medium without any carbon source (Fig. 4).

Upon transfer of methanol-grown cells to glucose medium, new small peroxisomes appeared that were not in contact with the vacuole (Fig. 4). Because glucose fully represses peroxisome proliferation and the synthesis of abundant peroxisomal enzymes, further organellar growth is not required at these conditions. The larger peroxisomes became much less abundant, possibly because they diluted out over the newly formed cells. However, the relatively large peroxisomes that still were present 2 h after the shift to glucose medium remained in contact with vacuoles (Fig. 4).

We previously reported that removal of Pex3 via the ubiquitin-proteasome pathway is an early stage in macropexophagy in *H. polymorpha* [33,34]. It is tempting to speculate that the Pex3 protein that localizes to peroxisome-vacuole contact sites cannot be ubiquitinated thereby preventing the autophagosome to engulf the organelle that associates to the vacuole.

Pex3 is a highly conserved peroxin that was initially described to play a role in PMP sorting. In this process, Pex3 binds Pex19, the receptor/chaperone for newly synthesized PMPs [35] (Fig. 6). Later studies revealed additional, unrelated functions for Pex3 at conditions that induce pexophagy (by binding *Pichia pastoris* Atg30 or *S. cerevisiae* Atg36 [36,37]) and in peroxisome retention in budding yeast cells (via the association of Inp1, [38]) (Fig. 6). Our current data add to the model that Pex3 represents an anchor protein at the peroxisomal membrane, which can recruit different components that play a role in a range of processes important in peroxisome biology. For the formation of peroxisome-vacuole contacts, Pex3 may bind a yet unknown protein. Alternatively, Pex3 may directly associate to the vacuolar membrane, which finds support in the observation that the cytosolic soluble domain of Pex3 has affinity for lipids [39].

Very recently peroxisome vacuole-contacts were detected in *S. cerevisiae* using split-GFP technology [16,40]. In these studies, different split-GFP fragments were constructed that sort to a range of organelle pairs, which allow visualizing organellar contact sites by FM. This approach offers a very attractive method to develop high-throughput screens for the identification of peroxisome-vacuole contact site proteins in *S. cerevisiae*.

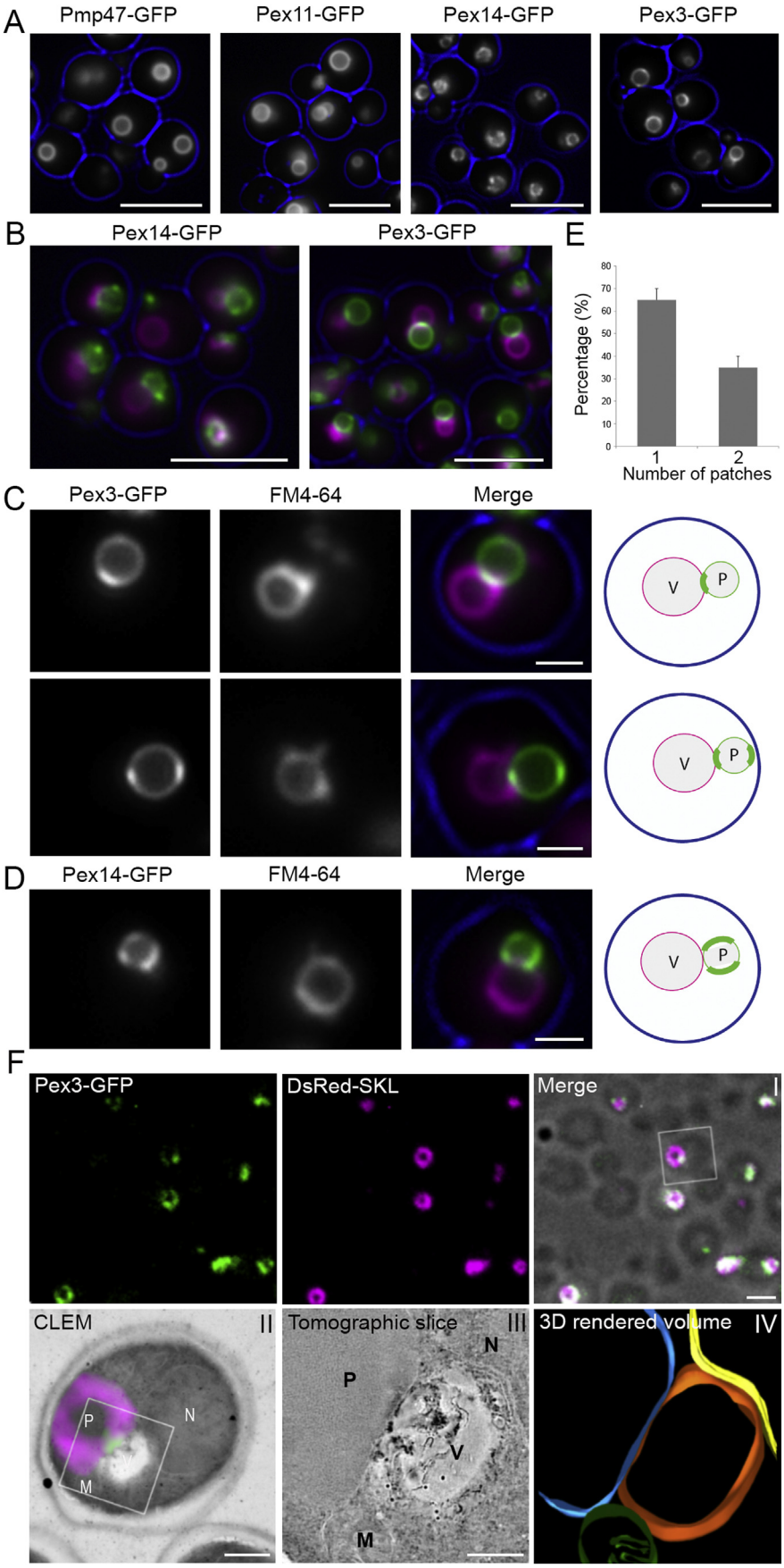

Fig. 3. Pex3 is enriched at peroxisome vacuole contacts in methanol-induced cells. **(A)** FM images of WT cells producing the indicated PMPs containing GFP at the C-terminus and produced under control of their endogenous promoters. Cells were induced for a few hours on methanol medium. **(B)** overview and **(C, D)** details of FM images of cells producing Pex14-GFP or Pex3-GFP stained with the vacuolar marker FM4–64 (purple) together with schematic representations of the regions where generally the GFP patches are observed for Pex3-GFP and Pex14-GFP. In the merged images, cell contours are indicated in blue. Scale bar 1 μm in C, D; 5 μm in A, B. **(E)** Quantification of the percentage of peroxisomes containing one or two Pex3-GFP patches. For quantifying Pex3-GFP patches, the signal intensity variation on the peroxisomal membrane was measured. A patch is defined as a region where the signal was 50% higher compared to the lowest signal measured on the same peroxisome.2 × 40 peroxisomes from two independent cultures were counted. Error bar represents SD. **(F)** Correlative light and electron microscopy of cells producing Pex3-GFP and the matrix marker DsRed-SKL. **I**, A 200 nm thick cryosection was first imaged by FM. Scale bar 1 μm. **II**, Merged EM and FM images of the region indicated in the merged images of I. Scale bar 500 nm. DsRed-SKL fluorescence is not observed in the center of the larger peroxisomes because of the presence of an alcohol oxidase crystalloid inside these organelles. III Tomographic slice of the region indicated in II showing the close association of the peroxisome and the vacuole membrane at the site where the Pex3-GFP patch was observed by FM. Scale bar 100 nm. IV 3D rendered volume of the tomogram shown in III. Blue: peroxisome; Orange: vacuole; Yellow: nucleus, Green: mitochondrion.

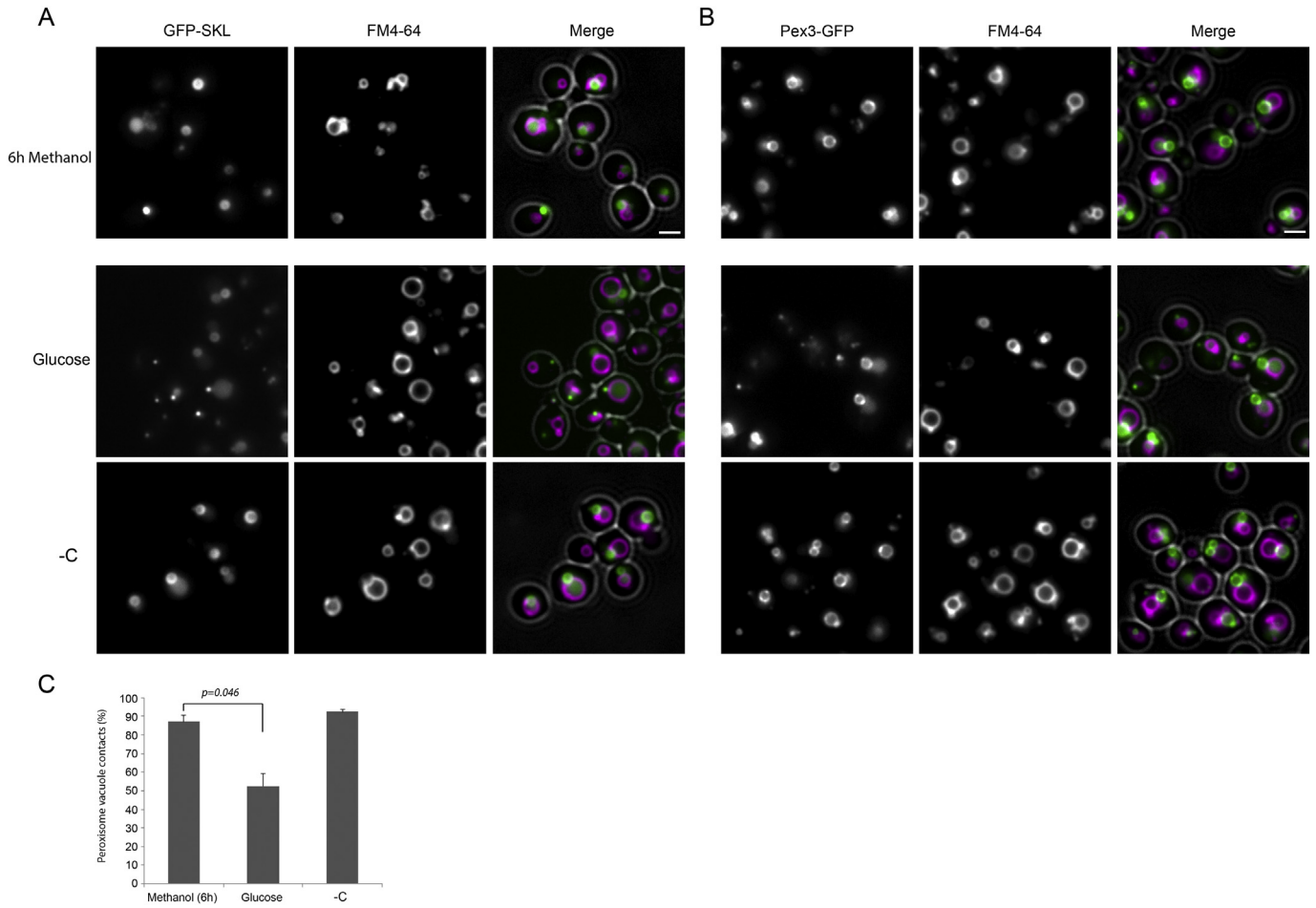

Fig. 4. The fate of peroxisome-vacuole contacts upon addition of glucose or removal of methanol. **(A, B)** FM images of cells producing GFP-SKL (A) or Pex3-GFP (B). Cells were precultivated for 6 h on methanol and subsequently shifted to glucose - containing medium (Glucose) or to medium without carbon source (−C). Cells were incubated for another 2 h and analyzed by fluorescence microscopy. Scale bar 2 µm. **(C)**) Percentage of peroxisomes that form peroxisome-vacuole contacts at the indicated growth conditions. GFP-SKL was used as a marker for peroxisomes and FM4–64 was used to stain the vacuolar membrane. Error bars represent standard deviation (SD). 2 × 140 peroxisomes of two independent cultures were used for the quantification. The *p* value was calculated by a t-test.

4. Materials and methods

4.1. Strains and growth conditions

The *H. polymorpha* strains used in this study are listed in Table S1. Yeast cells were grown in batch cultures at 37 °C on mineral medium (MM) [41] supplemented with 0.5% glucose or 0.5% methanol as carbon sources and 0.25% ammonium sulfate or 0.25% methylamine as nitrogen sources. When required, amino acids were added to the media to a final concentration of 30 µg/mL. For selection of transformants, plates were prepared containing 2% granulated agar and 0.67% yeast nitrogen base without amino acids (YNB; Difco; BD) containing 0.5% glucose or YPD (1% yeast extract, 1% peptone, and 1% glucose) supplemented with 100 µg/mL zeocin (Invitrogen).

4.2. Construction of H. polymorpha strains

All plasmids and oligonucleotide primers used in this study are listed in Tables S2. Transformation and site-specific integration were performed as described previously [42].

To construct an *H. polymorpha* WT strain overproducing Pex14-eGFP (under control of the amine oxidase promoter, P_{AMO}), plasmid pHIPX5 Pex14-eGFP was linearized with *Bsu*36I and integrated into the genome of *H. polymorpha yku80*.

In order to obtain plasmid pHIPX5 Pex14-eGFP, the Pex14-eGFP fragment was digested from the plasmid pHIPX4 Pex14-eGFP (gift from Masayuki Komori) using *Bam*HI and *Sac*I. Then the fragment was inserted between *Bam*HI and *Sac*I sites of the plasmid pHIPX5 [43].

Plasmid pHIPZ Pex14-mGFP (pSNA12, [25] was linearized with *Pst*I and integrated into the genome of *H. polymorpha* NCYC495, resulting in a strain producing Pex14-mGFP under control of its own promoter.

Plasmid pHIPZ Pex3-mGFP (designated pSEM61) was obtained as follows: PCR was performed on *H. polymorpha* WT genomic DNA using primers Pex3-F and Pex3-R. The PCR product was digested with *Hin*dIII and *Bgl*II. Then the resulting fragment was inserted between the *Hin*dIII and *Bgl*II sites of the pHIPZ mGFP fusinator plasmid [44]. *Eco*RI-linearized pSEM61 was integrated into the *PEX3* gene of *H. polymorpha yku80* producing DsRed-SKL, resulting in a strain producing Pex3-GFP under control of its own promoter. Moreover, *H. polymorpha yku80* producing DsRed-SKL was constructed upon the integration of *Nsi*I-linearized pHIPN4 DsRed-SKL (Cepinska et al., 2011) into the genomic DNA.

4.3. Biochemical techniques

Total cell extracts were prepared for western blot analysis upon TCA precipitation of whole cells as described before [45]. Equal amounts of protein were loaded per lane. Western blots were probed with mouse monoclonal antiserum against GFP (sc-9996; Santa Cruz Biotechnology, Inc.), rabbit polyclonal antisera against pyruvate carboxylase-1 (Pyc1

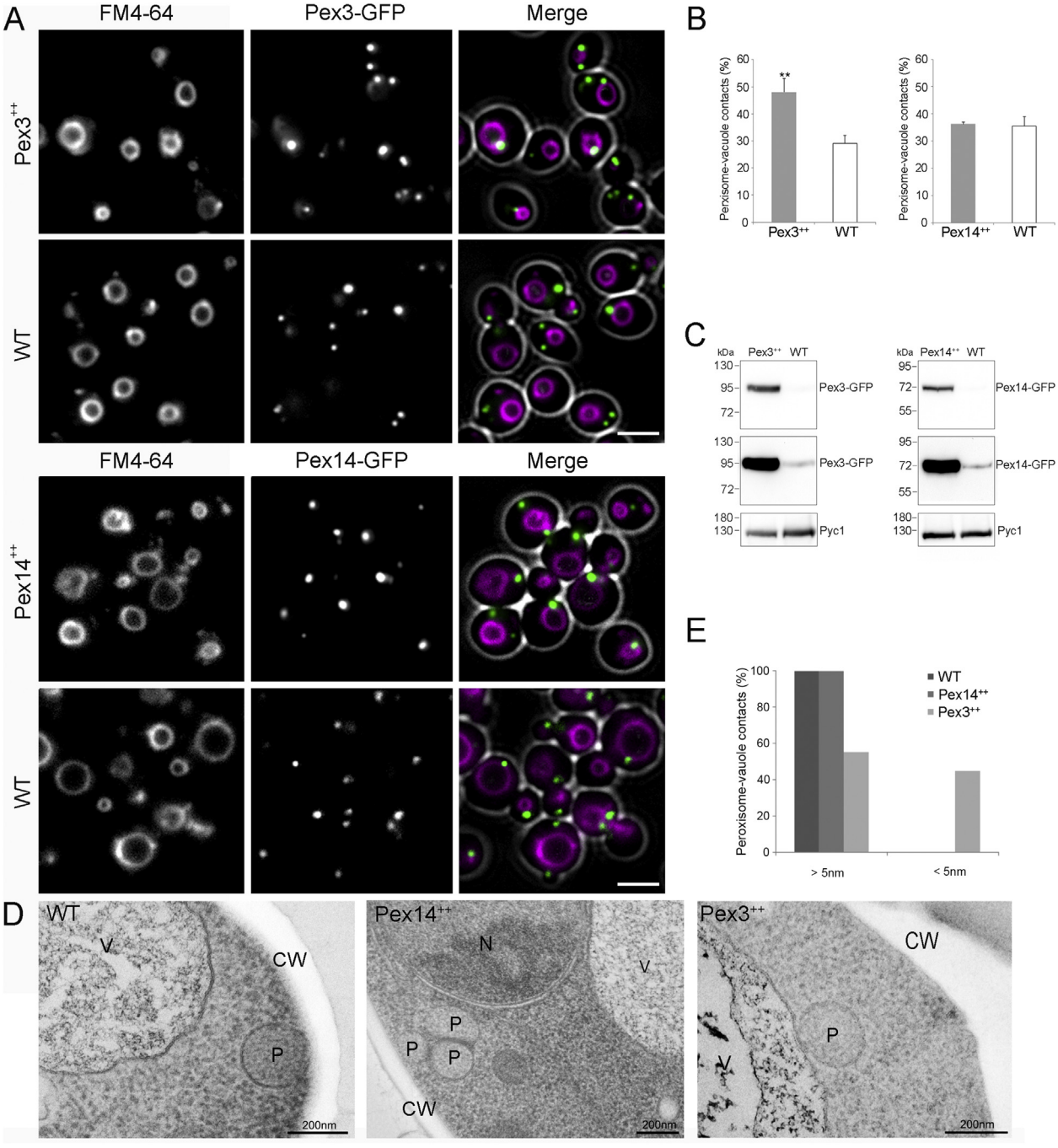

Fig. 5. Modulation of the Pex3 levels affects peroxisome-vacuole contact sites. (A) FM images of glucose/methylamine-grown cells producing Pex3-GFP under control of the P_{AMO} ($Pex3^{++}$) or P_{PEX3} (WT) or Pex14-GFP under control of the P_{AMO} ($Pex14^{++}$) or P_{PEX14} (WT). Scale bar 2.5 µm. (B) Quantification of the percentage of Pex3-GFP or Pex14-GFP spots co-localizing with the vacuolar marker FM4–64. The percentage of Pex3-GFP or Pex14-GFP patches that overlapped with red fluorescence from the vacuolar marker FM4–64 was calculated from two independent cultures (200 cells per culture). Error bars represent SD. Asterisks indicate significant difference (**$p < 0.01$), t-test. (C) Immunoblots demonstrating enhanced levels of Pex3-GFP in the $Pex3^{++}$ strain or Pex14-GFP in the $Pex14^{++}$ strain. Equal amounts of cell extracts were loaded per lane. Blots were decorated with α-GFP or α-pyruvate carboxylase (Pyc1) antibodies. Pyc1 was used as a loading control. Exposure times of GFP blot: 20 s (upper panel) and 200 s (lower panel). (D) EM analysis of the identical cells as shown in A. CW: cell wall, M: mitochondrion, P: peroxisome, N: nucleus, V: vacuole. Scale bar: 200 nm. (E) Quantitative analysis of the percentage of peroxisomes that have a contact site with the vacuole (distance between membranes < 5 nm) in WT, $Pex3^{++}$ or $Pex14^{++}$ cells. The percentages were calculated from the analysis of 29 individual peroxisomes per strain.

[46], Pex11 [47], Pex14 [48] or Pex3 [49]. Secondary goat anti-rabbit or goat anti-mouse antibodies conjugated to horseradish peroxidase (Thermo Fisher Scientific) were used for detection. Pyc1 was used as a loading control.

4.4. Fluorescence microscopy

Widefield images were captured at room temperature using a 100 × 1.30 NA objective (Carl Zeiss, Oberkochen, Germany). Images were obtained from the cells in growth media using a Zeiss Axioscope A1 fluorescence microscope (Carl Zeiss, Oberkochen, Germany), Micro-Manager 1.4 software and a CoolSNAP HQ^2 camera. The GFP

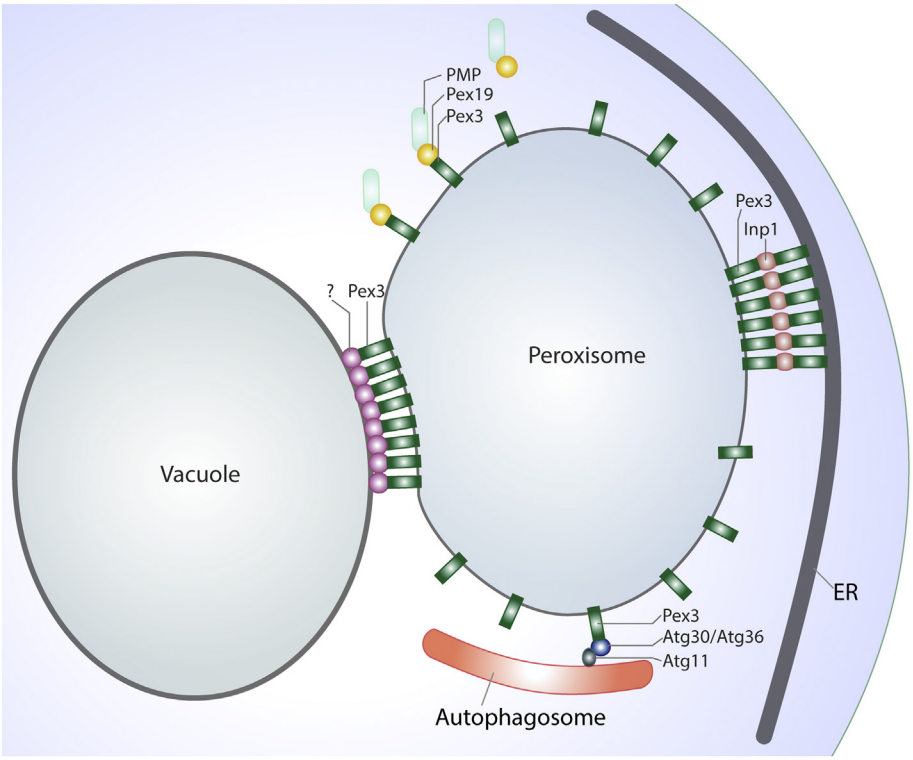

Fig. 6. Pex3 plays a role in various processes important in peroxisome biology. Schematic representation of different proposed functions of Pex3 in peroxisome biology. These include PMP sorting, pexophagy, peroxisome retention and vacuole contact site formation.

fluorescence was visualized with a 470/40 nm bandpass excitation filter, a 495 nm dichromatic mirror, and a 525/50 nm band-pass emission filter. FM4–64 fluorescence was visualized with a 546/12 nm bandpass excitation filter, a 560 nm dichromatic mirror, and a 575–640 nm bandpass emission filter. The vacuolar membranes were stained with FM4–64 (Invitrogen) by incubating cells at 37 °C with 2 μM FM4–64. Image analysis was performed using ImageJ and Adobe Photoshop CC software.

For quantifying Pex3-GFP patches, the signal intensity variation on the peroxisomal membrane was measured. When the signal was 50% higher compared to the lowest signal measured on the same peroxisome, it was considered to be a patch. The percentage of peroxisomes containing a patch was calculated from two biological replicates containing each 40 peroxisomes. The signal variation of Pex11-GFP and Pmp47-GFP on a single peroxisome was on average < 25%. The error bars indicate the standard deviation.

Peroxisome-vacuole contacts were defined as regions where green fluorescence signals (from GFP-SKL or Pex3-GFP) overlapped with red fluorescence from FM4–64. The percentage of peroxisomes forming a contact with vacuoles was calculated from two biological replicates. The error bars indicate the standard deviation.

4.5. Electron microscopy (EM)

For morphological analysis, cells were fixed in 1.5% potassium permanganate, post-stained with 0.5% uranyl acetate, and embedded in Epon. For cryofixation, cells were fixed using self-pressurized rapid freezing [50]. The copper capillaries were sliced open longitudinally and placed on frozen freeze-substitution medium containing 1% osmium tetroxide, 0.5% uranyl acetate and 5% water in acetone. The tube fragments containing cell material were dehydrated and fixed using the rapid freeze substitution method [51]. Samples were embedded in Epon and ultra-thin sections were collected on formvar-coated and carbon evaporated copper grids and inspected using a CM12 (Philips) transmission electron microscope (TEM).

For quantification of membrane contacts, ribbons of 60 nm thick sections from chemically fixed cells were collected on Formvar-coated and carbon evaporated single-hole grids. Entire peroxisomes were imaged in serial sections. The maximum length of a contact size and the number of contacts were measured using ImageJ.

Correlative light and electron microscopy (CLEM) was performed using cryosections as described previously [52]. Sections were imaged on an Observer Z1 (Carl Zeiss) fluorescence microscope with a 63 × 1.25 NA Plan-Neofluar objective (Carl Zeiss) equipped with an AxioCAM MRm camera (Carl Zeiss) using Zen 2.3 software. GFP fluorescence was visualized with a 470/40-nm bandpass excitation filter, a 495 nm dichromatic mirror, and a 525/50 nm band-pass emission filter. DsRed fluorescence was visualized with a 546/12-nm bandpass excitation filter, a 560-nm dichromatic mirror, and a 575–640-nm bandpass emission filter. After fluorescence imaging, the grid was post-stained and embedded in a mixture of 0.5% uranyl acetate and 0.5% methylcellulose. Acquisition of the double-tilt tomography series for CLEM was performed manually in a CM12 TEM running at 90 kV and included a tilt range of 40° to −40 with 2.5° increments. To construct the CLEM images, pictures taken with FM and EM were aligned using the eC-CLEM plugin [53] in Icy (http://icy.bioimageanalysis.org). Reconstruction of the tomograms was performed using the IMOD software package.

Transparency document

The Transparency document associated with this article can be found, in online version.

Acknowledgments

We thank Cornelieke Werkman for assistance in strain construction. This work was supported by grants from the CHINA SCHOLARSHIP COUNCIL to HW and YW, the Netherlands Organisation for Scientific Research/Chemical Sciences (NWO/CW) to AA (711.012.002) and the

Marie Curie Initial Training Networks (ITN) program PerFuMe (Grant Agreement Number 316723) to IvdK.

The authors declare no competing financial interests.Author contributions

Arjen M. Krikken, Rinse de Boer, Arman Akşit, Yuan Wei and Ida J. van der Klei conceived the project. Huala Wu, Arjen Krikken and Rinse de Boer performed the experiments, analyzed the data and prepared the figures. Ida J. van der Klei wrote the original draft. Huala Wu, Rinse de Boer, Arjen M. Krikken, Arman Akşit and Yuan Wei contributed to reviewing and editing the manuscript.

Appendix A. Supplementary data

Supplementary data to this article can be found online at https://doi.org/10.1016/j.bbamcr.2018.08.021.

References

[1] S. Lahiri, A. Toulmay, W.A. Prinz, Membrane contact sites, gateways for lipid homeostasis, Curr. Opin. Cell Biol. 33 (2015) 82–87.
[2] T. Burgoyne, S. Patel, E.R. Eden, Calcium signaling at ER membrane contact sites, Biochim. Biophys. Acta 1853 (2015) 2012–2017.
[3] W.A. Prinz, Bridging the gap: membrane contact sites in signaling, metabolism, and organelle dynamics, J. Cell Biol. 205 (2014) 759–769.
[4] N. Shai, M. Schuldiner, E. Zalckvar, No peroxisome is an island - peroxisome contact sites, Biochim. Biophys. Acta 1863 (2016) 1061–1069.
[5] J.J. Smith, J.D. Aitchison, Peroxisomes take shape, Nat. Rev. Mol. Cell Biol. 14 (2013) 803–817.
[6] M. Schrader, L.F. Godinho, J.L. Costello, M. Islinger, The different facets of organelle interplay-an overview of organelle interactions, Front. Cell Dev. Biol. 3 (2015) 56.
[7] J.L. Costello, I.G. Castro, T.A. Schrader, M. Islinger, M. Schrader, Peroxisomal ACBD4 interacts with VAPB and promotes ER-peroxisome associations, Cell Cycle 16 (2017) 1039–1045.
[8] R. Hua, D. Cheng, E. Coyaud, S. Freeman, E. Di Pietro, Y. Wang, A. Vissa, C.M. Yip, G.D. Fairn, N. Braverman, J.H. Brumell, W.S. Trimble, B. Raught, P.K. Kim, VAPs and ACBD5 tether peroxisomes to the ER for peroxisome maintenance and lipid homeostasis, J. Cell Biol. 216 (2017) 367–377.
[9] B. Knoblach, X. Sun, N. Coquelle, A. Fagarasanu, R.L. Poirier, R.A. Rachubinski, An ER-peroxisome tether exerts peroxisome population control in yeast, EMBO J. 32 (2013) 2439–2453.
[10] M. Fagarasanu, A. Fagarasanu, Y.Y. Tam, J.D. Aitchison, R.A. Rachubinski, Inp1p is a peroxisomal membrane protein required for peroxisome inheritance in Saccharomyces cerevisiae, J. Cell Biol. 169 (2005) 765–775.
[11] C. David, J. Koch, S. Oeljeklaus, A. Laernsack, S. Melchior, S. Wiese, A. Schummer, R. Erdmann, B. Warscheid, C. Brocard, A combined approach of quantitative interaction proteomics and live-cell imaging reveals a regulatory role for endoplasmic reticulum (ER) reticulon homology proteins in peroxisome biogenesis, Mol. Cell. Proteomics 12 (2013) 2408–2425.
[12] A.S. Joshi, X. Huang, V. Choudhary, T.P. Levine, J. Hu, W.A. Prinz, A family of membrane-shaping proteins at ER subdomains regulates pre-peroxisomal vesicle biogenesis, J. Cell Biol. 215 (2016) 515–529.
[13] F.D. Mast, A. Jamakhandi, R.A. Saleem, D.J. Dilworth, R.S. Rogers, R.A. Rachubinski, J.D. Aitchison, Peroxins Pex30 and Pex29 dynamically associate with reticulons to regulate peroxisome biogenesis from the endoplasmic reticulum, J. Biol. Chem. 291 (2016) 15408–15427.
[14] Y. Cohen, Y.A. Klug, L. Dimitrov, Z. Erez, S.G. Chuartzman, D. Elinger, I. Yofe, K. Soliman, J. Gartner, S. Thoms, R. Schekman, Y. Elbaz-Alon, E. Zalckvar, M. Schuldiner, Peroxisomes are juxtaposed to strategic sites on mitochondria, Mol. BioSyst. 10 (2014) 1742–1748.
[15] M. Mattiazzi Usaj, M. Brloznik, P. Kaferle, M. Zitnik, H. Wolinski, F. Leitner, S.D. Kohlwein, B. Zupan, U. Petrovic, Genome-wide localization study of yeast Pex11 identifies peroxisome-mitochondria interactions through the ERMES complex, J. Mol. Biol. 427 (2015) 2072–2087.
[16] N. Shai, E. Yifrach, C.W.T. van Roermund, N. Cohen, C. Bibi, I.J. L, L. Cavellini, J. Meurisse, R. Schuster, L. Zada, M.C. Mari, F.M. Reggiori, A.L. Hughes, M. Escobar-Henriques, M.M. Cohen, H.R. Waterham, R.J.A. Wanders, M. Schuldiner, E. Zalckvar, Systematic mapping of contact sites reveals tethers and a function for the peroxisome-mitochondria contact, Nat. Commun. 9 (2018) 1761.
[17] W.A. Dunn Jr., J.M. Cregg, J.A. Kiel, I.J. van der Klei, M. Oku, Y. Sakai, A.A. Sibirny, O.V. Stasyk, M. Veenhuis, Pexophagy: the selective autophagy of peroxisomes, Autophagy 1 (2005) 75–83.
[18] A.L. Anding, E.H. Baehrecke, Cleaning house: selective autophagy of organelles, Dev. Cell 41 (2017) 10–22.
[19] M. Veenhuis, J.P. van Dijken, S.A. Pilon, W. Harder, Development of crystalline peroxisomes in methanol-grown cells of the yeast *Hansenula polymorpha* and its relation to environmental conditions, Arch. Microbiol. 117 (1978) 153–163.
[20] S. Raychaudhuri, W.A. Prinz, Nonvesicular phospholipid transfer between peroxisomes and the endoplasmic reticulum, Proc. Natl. Acad. Sci. U. S. A. 105 (2008) 15785–15790.
[21] V.V. Flis, A. Fankl, C. Ramprecht, G. Zellnig, E. Leitner, A. Hermetter, G. Daum, Phosphatidylcholine supply to peroxisomes of the yeast *Saccharomyces cerevisiae*, PLoS One 10 (2015) e0135084.
[22] S. Rosenberger, M. Connerth, G. Zellnig, G. Daum, Phosphatidylethanolamine synthesized by three different pathways is supplied to peroxisomes of the yeast *Saccharomyces cerevisiae*, Biochim. Biophys. Acta 1791 (2009) 379–387.
[23] M. Veenhuis, I. Keizer, W. Harder, Characterization of peroxisomes in glucose-grown *Hansenula polymorpha* and their development after the transfer of cells into methanol-containing media, Arch. Microbiol. 120 (1979) 167–175.
[24] A.R. Bellu, A.M. Kram, J.A. Kiel, M. Veenhuis, I.J. van der Klei, Glucose-induced and nitrogen-starvation-induced peroxisome degradation are distinct processes in *Hansenula polymorpha* that involve both common and unique genes, FEMS Yeast Res. 1 (2001) 23–31.
[25] M.N. Cepinska, M. Veenhuis, I.J. van der Klei, S. Nagotu, Peroxisome fission is associated with reorganization of specific membrane proteins, Traffic 12 (2011) 925–937.
[26] W.F. Visser, C.W. van Roermund, L. Ijlst, H.R. Waterham, R.J. Wanders, Metabolite transport across the peroxisomal membrane, Biochem. J. 401 (2007) 365–375.
[27] M. Schrader, J.L. Costello, L.F. Godinho, A.S. Azadi, M. Islinger, Proliferation and fission of peroxisomes - an update, Biochim. Biophys. Acta 1863 (2016) 971–983.
[28] K. Zwart, M. Veenhuis, J.P. van Dijken, W. Harder, Development of amine oxidase-containing peroxisomes in yeasts during growth on glucose in the presence of methylamine as the sole source of nitrogen, Arch. Microbiol. 126 (1980) 117–126.
[29] M. Veenhuis, A. Douma, W. Harder, M. Osumi, Degradation and turnover of peroxisomes in the yeast *Hansenula polymorpha* induced by selective inactivation of peroxisomal enzymes, Arch. Microbiol. 134 (1983) 193–203.
[30] Y. Elbaz-Alon, E. Rosenfeld-Gur, V. Shinder, A.H. Futerman, T. Geiger, M. Schuldiner, A dynamic interface between vacuoles and mitochondria in yeast, Dev. Cell 30 (2014) 95–102.
[31] C. Ungermann, vCLAMPs-an intimate link between vacuoles and mitochondria, Curr. Opin. Cell Biol. 35 (2015) 30–36.
[32] C. Honscher, M. Mari, K. Auffarth, M. Bohnert, J. Griffith, W. Geerts, M. van der Laan, M. Cabrera, F. Reggiori, C. Ungermann, Cellular metabolism regulates contact sites between vacuoles and mitochondria, Dev. Cell 30 (2014) 86–94.
[33] A.R. Bellu, F.A. Salomons, J.A. Kiel, M. Veenhuis, I.J. Van Der Klei, Removal of Pex3p is an important initial stage in selective peroxisome degradation in *Hansenula polymorpha*, J. Biol. Chem. 277 (2002) 42875–42880.
[34] C. Williams, I.J. van der Klei, Pexophagy-linked degradation of the peroxisomal membrane protein Pex3p involves the ubiquitin-proteasome system, Biochem. Biophys. Res. Commun. 438 (2013) 395–401.
[35] Y. Fujiki, Y. Matsuzono, T. Matsuzaki, M. Fransen, Import of peroxisomal membrane proteins: the interplay of Pex3p- and Pex19p-mediated interactions, Biochim. Biophys. Acta 1763 (2006) 1639–1646.
[36] S.F. Burnett, J.C. Farre, T.Y. Nazarko, S. Subramani, Peroxisomal Pex3 activates selective autophagy of peroxisomes via interaction with the pexophagy receptor Atg30, J. Biol. Chem. 290 (2015) 8623–8631.
[37] A.M. Motley, J.M. Nuttall, E.H. Hettema, Pex3-anchored Atg36 tags peroxisomes for degradation in *Saccharomyces cerevisiae*, EMBO J. 31 (2012) 2852–2868.
[38] B. Knoblach, R.A. Rachubinski, Doing the math: how yeast cells maintain their peroxisome populations, Commun. Integr. Biol. 6 (2013) e26901.
[39] M.P. Pinto, C.P. Grou, M. Fransen, C. Sa-Miranda, J.E. Azevedo, The cytosolic domain of PEX3, a protein involved in the biogenesis of peroxisomes, binds membrane lipids, Biochim. Biophys. Acta 1793 (2009) 1669–1675.
[40] Y. Kakimoto, S. Tashiro, R. Kojima, Y. Morozumi, T. Endo, Y. Tamura, Visualizing multiple inter-organelle contact sites using the organelle-targeted split-GFP system, Sci. Rep. 8 (2018) 6175.
[41] J.P. van Dijken, R. Otto, W. Harder, Growth of *Hansenula polymorpha* in a methanol-limited chemostat. Physiological responses due to the involvement of methanol oxidase as a key enzyme in methanol metabolism, Arch. Microbiol. 111 (1976) 137–144.
[42] K.N. Faber, P. Haima, W. Harder, M. Veenhuis, G. Ab, Highly-efficient electrotransformation of the yeast *Hansenula polymorpha*, Curr. Genet. 25 (1994) 305–310.
[43] J.A. Kiel, I.K. Keizer-Gunnink, T. Krause, M. Komori, M. Veenhuis, Heterologous complementation of peroxisome function in yeast: the Saccharomyces cerevisiae PAS3 gene restores peroxisome biogenesis in a *Hansenula polymorpha* per9 disruption mutant, FEBS Lett. 377 (1995) 434–438.
[44] R. Saraya, M.N. Cepinska, J.A. Kiel, M. Veenhuis, I.J. van der Klei, A conserved function for Inp2 in peroxisome inheritance, Biochim. Biophys. Acta 1803 (2010) 617–622.
[45] R.J. Baerends, K.N. Faber, A.M. Kram, J.A. Kiel, I.J. van der Klei, M. Veenhuis, A stretch of positively charged amino acids at the N terminus of *Hansenula polymorpha* Pex3p is involved in incorporation of the protein into the peroxisomal membrane, J. Biol. Chem. 275 (2000) 9986–9995.
[46] P. Ozimek, R. van Dijk, K. Latchev, C. Gancedo, D.Y. Wang, I.J. van der Klei, M. Veenhuis, Pyruvate carboxylase is an essential protein in the assembly of yeast peroxisomal oligomeric alcohol oxidase, Mol. Biol. Cell 14 (2003) 786–797.
[47] A.M. Krikken, M. Veenhuis, I.J. van der Klei, *Hansenula polymorpha* pex11 cells are affected in peroxisome retention, FEBS J. 276 (2009) 1429–1439.
[48] M. Komori, S.W. Rasmussen, J.A. Kiel, R.J. Baerends, J.M. Cregg, I.J. van der Klei, M. Veenhuis, The *Hansenula polymorpha* PEX14 gene encodes a novel peroxisomal membrane protein essential for peroxisome biogenesis, EMBO J. 16 (1997) 44–53.
[49] R.J. Baerends, S.W. Rasmussen, R.E. Hilbrands, M. van der Heide, K.N. Faber, P.T. Reuvekamp, J.A. Kiel, J.M. Cregg, I.J. van der Klei, M. Veenhuis, The *Hansenula polymorpha* PER9 gene encodes a peroxisomal membrane protein essential for peroxisome assembly and integrity, J. Biol. Chem. 271 (1996) 8887–8894.
[50] J.L. Leunissen, H. Yi, Self-pressurized rapid freezing (SPRF): a novel cryofixation

method for specimen preparation in electron microscopy, J. Microsc. 235 (2009) 25–35.
[51] K.L. McDonald, R.I. Webb, Freeze substitution in 3 hours or less, J. Microsc. 243 (2011) 227–233.
[52] K. Knoops, R. de Boer, A. Kram, I.J. van der Klei, Yeast pex1 cells contain peroxisomal ghosts that import matrix proteins upon reintroduction of Pex1, J. Cell Biol. 211 (2015) 955–962.
[53] P. Paul-Gilloteaux, X. Heiligenstein, M. Belle, M.C. Domart, B. Larijani, L. Collinson, G. Raposo, J. Salamero, eC-CLEM: flexible multidimensional registration software for correlative microscopies, Nat. Methods 14 (2017) 102–103.